Nanostructured Gas Diffusion and Catalyst Layers for Proton Exchange Membrane Fuel Cells

Arunachala M. Kannan,[a,*,z] Vinod P. Veedu,[b] Lakshmi Munukutla,[a] and Mehrdad N. Ghasemi-Nejhad[b]

[a]*Department of Electronic Systems, Arizona State University at the Polytechnic Campus, Mesa, Arizona 85212, USA*
[b]*Hawaii Nanotechnology Laboratories, Department of Mechanical Engineering, University of Hawaii at Manoa, Honolulu, Hawaii 96822, USA*

Nanostructured components are introduced in membrane electrodes assembly (MEA) in proton exchange membrane fuel cell as a solution to improve the performance. Single-walled carbon nanotubes and multiwalled carbon nanotubes supported platinum are used to fabricate the gas diffusion layer (GDL) and the catalyst layers in the MEAs, respectively. The physicochemical and electrochemical characterizations of these nanotube-based components demonstrate excellent GDL surface morphology and uniform distribution of the platinum catalyst over the carbon nanotube support. The fuel cell testing using these nanostructured components exhibits promising fuel cell performance using hydrogen-air and hydrogen-oxygen at ambient pressure.
© 2006 The Electrochemical Society. [DOI: 10.1149/1.2422751] All rights reserved.

Proton exchange membrane fuel cells (PEMFCs) attract considerable interest as alternative power sources for low or zero emission vehicles as well as for stationary and portable applications due to their higher power densities and environmental aptness.[1,2] However, commercialization of PEMFC systems are constrained by factors such as attaining maximum utilization of the platinum metal catalysts, and limited performance and durability associated with the membrane electrode assemblies.[3,4] Previous attempts to use carbon nanotubes as the platinum catalyst support did not succeed due to the lack of control of the particle size[5] to meet performance expectation of the PEMFC. Generally, the low catalyst activity[6] and mass transportation, mainly at the cathode, limit the power density values in PEMFCs. To date, efforts in improving the PEMFC performance have been focused through maximizing catalyst utilization by decreasing the catalyst nanoparticles on the carbon support, dispersing the platinum nanoparticles on the support uniformly, and also by enhancing proton transport using a polymer electrolyte within the catalyst layer.[7-9] With an objective to lower the cost, other electrocatalysts such as metal porphyrins,[10] metal oxides,[11,12] and ruthenium-based chalcogenides[13,14] have been pursued in the literature over the years; however, their electrocatalytic activities are generally inferior to that of pure platinum. Therefore, a major breakthrough is desired to achieve superior performance and durability demanded for commercial viability of PEMFCs.[4]

Gas diffusion layers (GDLs) are one of the major components of PEMFC that play a significant role on hydrogen-air system performance at high current density region.[15] Hence, it is important to have a GDL with optimized pore size and gas transport characteristics to attain best performance of the fuel cell. The superior mechanical and electrical properties of carbon nanotubes[16-19] offer both mechanical robustness (to provide durability) and improved performance of the PEMFC by using them as catalysts support in the catalyst layer. More recently, Kongkanand et al. and Girishkumar et al. reported synthesis and characterization of Pt and Pt-Ru alloy on single-walled carbon nanotubes (SWCNTs) toward PEMFCs and direct methanol fuel cell (DMFC) applications.[20-22] However, earlier studies do not provide sufficient evidence of an improved performance in the actual PEMFCs fabricated using carbon nanotubes either due to the lack of control of the size of the catalyst over nanotube support or due to meager distribution of the catalysts over the nanotube surface.[5,20-26] Here, we demonstrate a simple approach in which both proper distribution of the platinum catalyst over the carbon nanotube support and optimized catalyst nanoparticle size is

obtained, while ensuring the maximum utilization of the catalyst in a fuel cell at the same time. Due to superior electrical properties, multiwalled carbon nanotubes (MWCNTs) serve as a good catalyst support material. The transmission electron microscope (TEM) images of the MWCNTs supported platinum electrocatalyst show uniform catalyst distribution with a particle size of about 6–8 nm. In the process of utilizing carbon nanotube components for PEMFCs, we have also developed GDLs with different weight percentage combinations of Pureblack and SWCNTs. The scanning electron microscope (SEM) images of the GDL microstructure show excellent surface morphology without any cracks on the microporous layer. The membrane electrode assembly (MEA) with SWCNT-based GDLs and MWCNTs supported Pt catalyst show power density as high as 0.8 W/cm^2 at 70°C using hydrogen-oxygen as reactants without any back-pressure.

Experimental

Three different types of GDLs were fabricated with different combinations of SWCNTs and Pureblack as microporous layers. The combinations used in this study are SWCNTs (CarboLex AP-grade), Pureblack carbon (grade 205-110 from Superior Graphite Co., Chicago, IL) and an equal weight percentage composite mixture of Pureblack and SWCNTs. To fabricate the microporous layers, slurries of different carbons with PTFE (Teflon) dispersion in a mixture of isopropanol and deionized water (80:20 volume ratio) were prepared by ultrasonication for 20 min followed by a magnetic stirring for about 2 h. Hydrophobic characteristic of the microporous layers made from the SWCNTs and graphitized carbon black grade Pureblack was provided by TE 3859 Teflon suspension (DuPont). The carbon loading for the microporous layer was approximately 3.5 mg/cm^2 and the PTFE content was 30 wt %. GDLs were fabricated with Teflonized nonwoven 7 mil carbon paper (P50T, Ballard Applied Materials) as the substrate. The slurry was applied on the carbon paper by microspraying method. Subsequently, carbon paper with microporous layer was heat treated by sintering at 350°C under vacuum for about an hour.

The pore size distribution of the GDLs was measured using PoreMaster-60 GT in both low and high-pressure modes by Hg intrusion method in a fixed speed mode. The surface morphology of the GDL samples was examined by JEOL JSM-5900LV scanning electron microscope. Catalyst coated membranes (CCM) with 5 cm^2 geometrically active area (catalyst layers) were fabricated with platinized carbon (46.4% Pt on carbon, TEC1050E, Tanaka Kikinzoku Kogyo KK, Japan), by a microspray method on Nafion-112 membrane, for evaluating the GDLs. The fuel cell testing was conducted first for selecting the best-performing microporous layer based

* Electrochemical Society Active Member.
z E-mail: amk@asu.edu

GDL, and then further testing was conducted to evaluate the newly fabricated MWCNTs supported catalyst layer based CCMs using the best-performing GDL.

Platinum catalyst deposition on MWCNTs was carried out as follows.[27,28] MWCNTs were uniformly dispersed in deionized water through ultrasonication and magnetic stirring. The dispersion was heated to about 70°C with continuous stirring operation. Chloroplatinic acid (1 wt % in deionized water) and sodium formate (1 M in deionized water) reducing agent were simultaneously added dropwise into the MWCNT dispersion to deposit Pt (20 wt %, based on the amount of chloroplatinic acid added) on MWCNTs. To fully grow the platinum nanoparticles on the MWCNTs the solution was continuously stirred for about 2 h at 70°C after the completion of the reaction. The platinized MWCNT was filtered through G4 glass frit crucible and the precipitate was thoroughly washed with boiling deionized water to completely remove sodium ions and finally rinsed with acetone. The MWCNT supported catalyst cake was then dried overnight at 100°C in air oven and heat treated in flowing argon atmosphere at 800°C for 3 h.

Homogeneously dispersed MWCNT supported platinum catalyst sample in methanol was applied on a lacy carbon grid to examine distribution and particle size of Pt by TEM using Philips CM200-FEG. Catalyst coated membrane was fabricated using MWCNTs supported platinum catalyst slurry in isopropanol or methanol using the microspray method on Nafion-112 membrane, for evaluating the fuel cell performance.[29] The homogeneity of the catalyst slurry appears to be better with methanol compared to that with isopropanol. The catalyst loadings on the anode and cathode sides were about 0.5 mg Pt/cm^2, respectively.

In fuel cell testing, the best-performing GDL in combination with the MWCNT catalyst support and the catalyst coated membrane were assembled by sandwiching them inside the test cell (Fuel Cell Technologies). Gas sealing was carried out using silicone coated fabric materials (Performance Plastics, CF1007) and with a uniform torque of 40 lb-in.[29] Cyclic voltammetry (CV) was carried out using PARSTAT for measuring electrochemically active surface area (ECA) of the MEAs. The test cell was equilibrated for about 2 h with humidified hydrogen and nitrogen gases at 70°C before the voltage scanning for CV measurement. Single-cell fuel cell performance was evaluated using Fuel Cell Technologies Test Station, at 70°C with H$_2$/air as well as H$_2$/O$_2$ under ambient pressure by galvanostatic polarization. The relative humidity of the reactant gases were maintained at 100% by controlling the humidity bottle temperatures.

Results and Discussion

Figure 1 shows SEM micrographs of microporous layers of GDLs fabricated using (a) SWCNT, (b) Pureblack carbon, and (c) Pureblack carbon and SWCNTs (50/50 wt %). The micrographs of GDLs showed homogeneous carbon distribution and crack-free microporous layer favoring uniform gas distribution. The surface morphology explains clearly the mechanical characteristics of the GDL reinforcement by the presence of carbon nanotubes in Fig. 1a and c. The nanotubes are not ordered and they are entangled both in and through the plane to provide structural integrity of the microporous layer to the GDL substrate.

Figure 1d compares the pore size distribution data measured by Hg porosimetry for SWCNTs, Pureblack carbon, and the 50–50 wt % mixture of Pureblack carbon and SWCNTs. For the GDL with SWCNTs in the microporous layer, all the pores are larger than 0.2 μm in diameter, whereas other samples also show pores with ~0.06 μm diameter. In addition, there are differences in pores with larger diameter. For example, the GDL with 50–50 wt % mixture of Pureblack carbon and SWCNTs shows only one type of pore diameter >100 μm, and this might lead to improved gas distribution characteristics compared to other compositions. In this context, the microporous layer of the GDL structure with favorable pore size distribution will have increased liquid water flux through the GDL with minimum flooding so as to have improved oxygen diffusion
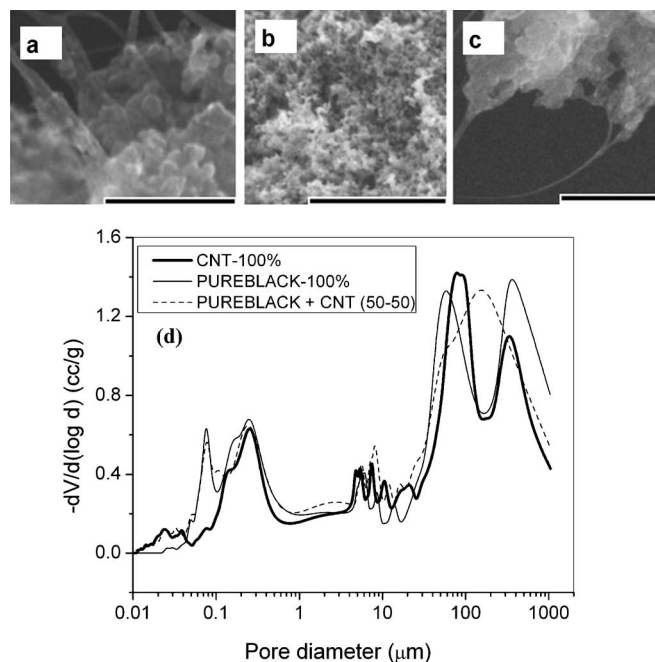

Figure 1. Fabricated GDLs and their pore size distribution. SEM images of microporous layers GDLs fabricated using (a) SWCNTs (scale bar = 300 nm); (b) Pureblack 205-110 carbon (scale bar = 5 μm); (c) Pureblack 205-110 carbon and SWCNTs (50/50 wt %) (scale bar = 500 nm); and (d) pore size distribution data for SWCNTs, Pureblack carbon, and Pureblack carbon and SWCNTs (50/50 wt %) using mercury porosimetry.

from gas channel to catalyst layer during fuel cell operation. Especially, when the cell is operating with 100% RH or at larger current density ranges (say >0.8 A/cm^2), the GDL with Pureblack carbon and SWCNTs (50–50 wt %) is expected to perform better compared to other composition of the microporous layers. Theoretical model and experimental results on liquid water flux and liquid saturation with varying pore diameter highlight the performance of the GDLs.[30-32]

Galvanostatic polarization data for MEAs at 70°C using SWCNTs, Pureblack carbon, and Pureblack carbon and SWCNTs (50–50 wt %) based GDLs with 7 mil macroporous carbon papers and Nafion-112 membrane as electrolyte with H$_2$ and air at ambient pressure are shown in Fig. 2. From Fig. 2, the combination of SWCNTs with Pureblack carbon based GDL with 7 mil carbon pa-
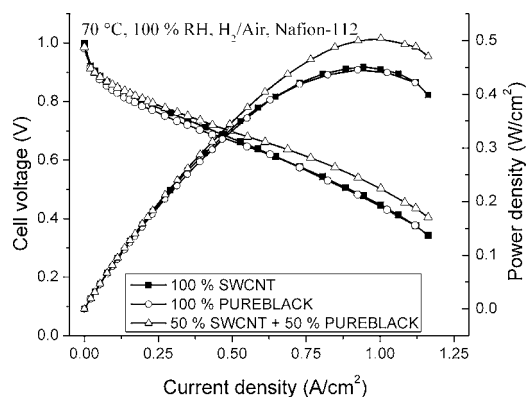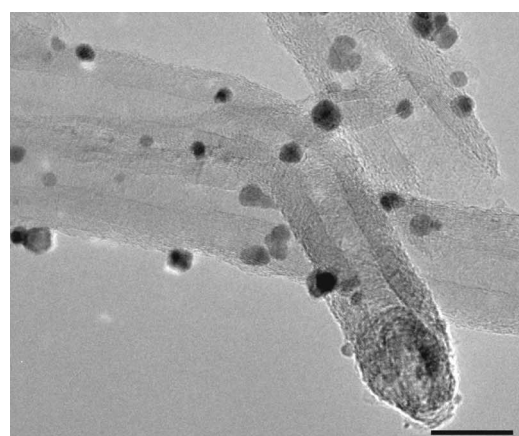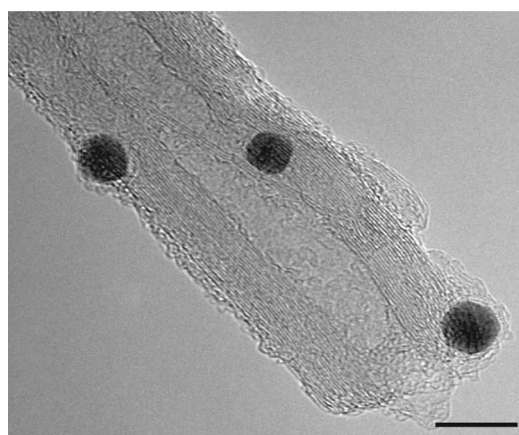

Figure 2. Galvanostatic polarization data for MEAs at 70°C using SWCNTs, Pureblack carbon, and Pureblack Carbon and SWCNTs (50/50 wt %) based GDLs with 7 mil macroporous carbon papers and Nafion-112 membrane as electrolyte with H$_2$/air at ambient pressure.

(a)

(b)

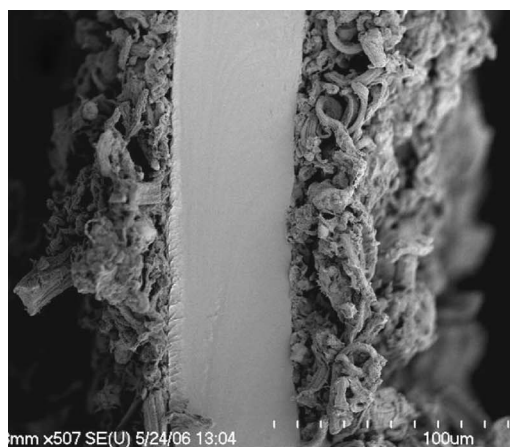**Figure 3.** TEM images of platinum supported on MWCNTs: (a) low magnification showing the chain structure (scale bar = 20 nm) and (b) high magnification showing well-defined platinum particles (scale bar = 10 nm).
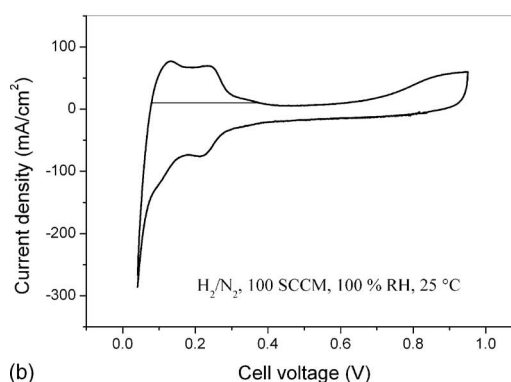

(a)

(b)

(c)

Figure 4. (a) SEM image for an MEA, fabricated by directly coating Nafion-112 with Pt/MWCNT catalyst by microspray technique. (b) CV data for an MEA, fabricated by directly coating Nafion 112 with Pt/MWCNT catalyst by microspray technique. (c) Galvanostatic polarization data for MEAs at 70°C using Pt/MWCNT catalyst in two different dispersion agents, with Pureblack 205-110 carbon and SWCNTs (50/50 wt %) based GDLs and Nafion-112 membrane as electrolyte with H_2/O_2 at ambient pressure.

per shows a power density value of ~ 0.5 W/cm^2 with hydrogen/air at ambient pressure. The enhanced power density value with H_2/air is attributed solely to the formation of favorable pores to minimize polarization loss and relatively better gas transport as well as water management characteristics especially at high current densities, in 100% RH operation.

Figures 3a and b show the high-resolution TEM images at two different magnifications of the new MWCNT supported platinum. It is evident from these figures that the Pt particles are uniformly distributed on the exterior sides of the carbon nanotubes. Figure 3b, taken at a higher magnification, depicts the presence of well-defined platinum particles in size ranges from 6 to 8 nm, without any agglomeration.
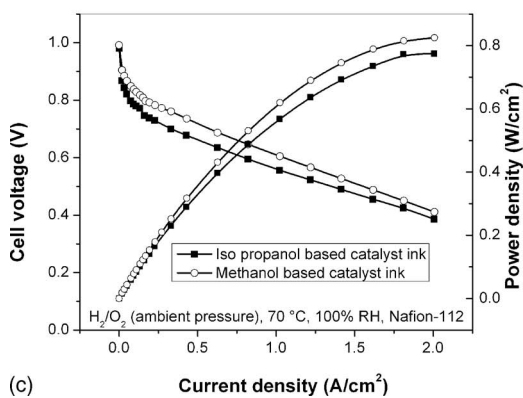
Figure 4a shows the cross-sectional view of a catalyst coated membrane using Nafion-112 membrane with Pt/MWCNT catalyst. As seen from this SEM micrograph, there is good interfacial continuity and integrity between the electrolyte surface and catalyst layer to minimize internal resistance, both on anode and cathode sides. Figure 4b shows the cyclic voltammogram of an MEA fabricated using MWCNT supported catalyst by the CCM process containing a loading of about 0.5 mg Pt/cm^2 on both anode and cathode. The ECA surface area calculated from the hydrogen desorption is about 63 m^2/g Pt. Figure 4c shows the fuel cell performance of a 5 cm^2 MEA at 70°C using Pt/MWCNT catalyst on anode and cathode with Pureblack carbon and SWCNTs (50–50 wt %) based GDLs and Nafion-112 membrane as electrolyte with H_2/O_2 at ambient pressure. The MEA in the present study using Pt on MWCNT catalyst at

ambient pressure shows excellent performance compared to that observed in the literature,[5] where the polarization data were reported with 2 atmosphere back-pressure. Figure 4c shows slightly higher performance (>0.6 V at 1 A/cm^2) at ambient pressure compared to the data (<0.6 V at 1 A/cm^2) at 1 atmosphere back-pressure using Pt/MWCNT reported by Liu et al.[33] The improved performance is due to the superior control on the dispersion and also particle size of platinum nanoparticles on the exterior of the MWCNTs. This study therefore clearly demonstrates the potentials for the use of SWCNTs and MWCNTs as nanodevice components in MEAs for PEMFCs.

Conclusions

SWCNT is demonstrated to be an effective microporous layer with and without Pureblack carbon for fabricating GDLs for PEMFC for 100% RH conditions. The GDL was characterized by physicochemical as well as electrochemical methods. The unique process developed for GDL fabrication exhibits excellent fuel cell performance using hydrogen/air at ambient pressure. In addition, Pt/MWCNT catalyst is developed by a wet chemistry route. High-resolution transmission electron micrographs show highly uniform distribution of platinum catalyst with a particle size of about 6–8 nm. The membrane electrode assembly with nanostructured components (Pt/MWCNT based catalyst and SWCNT based GDLs) shows power density of as high as 0.8 W/cm^2 at 70°C using hydrogen/oxygen at ambient pressure. The power density observed in the present study with Pt/MWCNT is superior compared with that reported due to the proper control on particle size and homogeneous distribution of platinum nanoparticles on carbon nanotubes.[5] The durability of Pt/MWCNT based MEAs along with SWCNT/Pureblack based GDLs deserves to be studied further.

Acknowledgments

References

1. R. Service, *Science*, **296**, 1222 (2002).
2. T. E. Springer, T. A. Zawodzinski, and S. Gottesfeld, *J. Electrochem. Soc.*, **138**, 2334 (1991).
3. M. F. Mathias, R. Makharia, H. A. Gasteiger, J. J. Conley, T. J. Fuller, C. J. Gittleman, S. S. Kocha, D. P. Miller, C. K. Mittelsteadt, T. Xie, S. G. Yan, and P. T. Yu, *Electrochem. Soc. Interface*, **14**(3), 24 (2005).
4. H. A. Gasteiger, S. S. Kocha, B. Sompalli, and F. T. Wagner, *Appl. Catal., B*, **56**, 9 (2005).
5. C. Wang, M. Waje, X. Wang, J. M. Tang, R. C. Haddon, and Y. S. Yan, *Nano Lett.*, **4**, 345 (2004).
6. S. D. Thompson, L. R. Jordan, and M. Forsyth, *Electrochim. Acta*, **46**, 1657 (2001).
7. X. Sun, R. Li, D. Villers, J. P. Dodelet, and S. Désilets, *Chem. Phys. Lett.*, **379**, 99 (2003).
8. K. Yasuda and Y. Nishimura, *Mater. Chem. Phys.*, **82**, 921 (2003).
9. C. H. Hsu and C. C. Wan, *J. Power Sources*, **115**, 268 (2003).
10. H. Liu, L. Zhang, J. Zhang, D. Ghosh, J. Jung, B. W. Downing, and E. Whittemore, *J. Power Sources*, In press.
11. J. Prakash, D. A. Tryk, W. Aldred, and E. B. Yeager, *J. Appl. Electrochem.*, **29**, 1463 (1999).
12. L. Jörissen, *J. Power Sources*, **155**, 23 (2006).
13. L. Zhang, J. Zhang, D. P. Wilkinson, and H. Wang, *J. Power Sources*, **156**, 171 (2006).
14. S. S. Ozenler and F. Kadirgan, *J. Power Sources*, **154**, 364 (2006).
15. A. L. Dicks, *J. Power Sources*, **156**, 128 (2006).
16. M. S. Dresselhaus, G. Dresselhaus, and P. C. Eklund, *Science of Fullerenes and Carbon Nanotubes*, Academic, San Diego (1996).
17. R. H. Baughman, A. A. Zakhidov, and W. A. de Heer, *Science*, **297**, 787 (2002).
18. R. S. Ruoff and D. C. Lorents, *Carbon*, **33**, 925 (1995).
19. M. Yu, O. Lourie, M. J. Dyer, K. Moloni, T. F. Kelly, and R. S. Ruoffet, *Science*, **287**, 637 (2000).
20. A. Kongkanand, S. Kuwabata, G. Girishkumar, and P. V. Kamat, *Langmuir*, **21**, 2392 (2006), and references cited therein.
21. A. Kongkanand, K. Vinodgopal, S. Kuwabata, and P. V. Kamat, *J. Phys. Chem. B*, **110**, 16185 (2006).
22. G. Girishkumar, T. D. Hall, K. Vinodgopal, and P. V. Kamat, *J. Phys. Chem. B*, **110**, 107 (2006), and references cited therein.
23. T. Matsumoto, T. Komatsu, H. Nakano, K. Arai, Y. Nagashima, E. Yoo, T. Yamazaki, M. Kijima, H. Shimizu, Y. Takasawa, and J. Nakamura, *Catal. Today*, **90**, 277 (2004).
24. W. Xin, W. Li, Z. Chena, M. Waje, and Y. Yan, *J. Power Sources*, **158**, 154 (2006).
25. Y. Shao, G. Yin, Y. Gao, and P. Shi, *J. Electrochem. Soc.*, **153**, A1093 (2006).
26. C. Kim, Y. J. Kim, Y. A. Kim, T. Yanagisawa, K. C. Park, and M. Endo, *J. Appl. Phys.*, **96**, 5903 (2004).
27. A. M. Kannan, A. K. Shukla, and A. Hamnett, *J. Appl. Electrochem.*, **8**, 149 (1988).
28. L. Xiong, A. M. Kannan, and A. Manthiram, *Electrochem. Commun.*, **4**, 898 (2002).
29. A. M. Kannan, A. Menghal, and I. Barsukov, *Electrochem. Commun.*, **8**, 887 (2006).
30. U. Pasaogullari and C. Y. Wang, *Electrochim. Acta*, **49**, 4359 (2004).
31. Z. Zhan, J. Xiao, D. Li, M. Pan, and R. Yuan, *J. Power Sources*, **160**, 1041 (2006).
32. M. V. Williams, E. Begg, L. Bonville, H. R. Kunz, and J. M. Fenton, *J. Electrochem. Soc.*, **151**, A1173 (2004).
33. Z. Liu, X. Lin, J. Y. Lee, W. Zhang, M. Han, and L. M. Gan, *Langmuir*, **18**, 4054 (2002).